Pyrolysis of n- octane at very low concentration and low temperature

N. Razafinarivo, R. Bounaceur, V. Burklé-Vitzthum, F. Lannuzel, R. Michels, G. Scacchi, P.M. M Marquaire

Pyrolysis of *n*-Octane at Very Low Concentration and Low Temperature

N. Razafinarivo [a,b], R. Bounaceur [a], V. Burklé-Vitzthum [a], F. Lannuzel [a,b], R. Michels [b], G. Scacchi [a], P.M. Marquaire [a]

[a] Laboratoire Réactions et Génie des Procédés, CNRS-UMR 7274, Université de Lorraine, ENSIC, 1 rue Grandville, BP 20451, F-54001 NANCY Cedex, France

[b] GeoRessources, CNRS-UMR 7359, Université de Lorraine, BP 70239, F-54501 Vandœuvre lès Nancy, France

Abstract

Hydrocarbon pyrolysis concerns many different fields (petroleum geochemistry, refinery, fuel thermal stability, pyrocarbon deposition, etc.). It is therefore studied in a wide variety of temperature-pressure experimental conditions, which strongly affect the chemistry of hydrocarbons cracking.

An experimental study of the pyrolysis of *n*-octane has been performed at very low reactant concentration (1 mbar diluted in inert gas - total pressure 1500 mbar - molar fraction 0.07%) in a closed reactor, at temperatures ranging between 350°C and 450°C, and reaction time from 1 h to 70 h. The major products of the reaction are 1-alkenes (C_2H_4 to C_7H_{14}), methane and ethane; other alkanes (C_3H_8 to C_6H_{14}) are minor products. At 450°C and 4 h, the conversion is close to 9% and we observe, in terms of molar fractions:

$$C_2H_4 > C_3H_6 \approx CH_4 > C_4H_8 > C_5H_{10} > C_6H_{12} \approx C_2H_6 > C_7H_{14}$$

These experimental results are very different from those of the thermal decomposition of *n*-alkanes at the same low temperature but at high pressure. In particular, the cracking stoichiometric equations (for example: $C_8H_{18} = C_6H_{14} + C_2H_4$) are not observed since alkanes

(except methane and ethane) are in very low quantities. This can be explained by the very low concentration of reactant which limits the bimolecular reactions. In our conditions, the radicals decompose several times by beta-scissions of C-C bonds when it is possible (unimolecular reaction), rather than react by H-transfers (metathesis) with the reactant (bimolecular reaction) which produce alkanes. A detailed free radical mechanism (184 reactions, 16 molecules and 18 radicals – mechanism available as Supplementary Material) allows modelling the experimental results.

Keywords

Pyrolysis, *n*-Octane, Thermal decomposition, High dilution of reactant, Kinetic modelling.

1. Introduction

Thermal chemistry of hydrocarbons during pyrolysis is important in many research fields as petroleum geochemistry [1-3], refining of crude oils, cracking of hydrocarbons to produce light olefins [4-7], thermal decomposition of endothermic jet fuels [8-10], conversion of coal and biomass to liquid fuels [11-14], depolymerization and recycling of synthetic polymers [15-17], pyrocarbon deposition for the elaboration of C/C composite materials [18-20], etc. The reaction conditions considered cover a very wide range of time and temperature, from 150°C during several millions of years in geochemistry studies, to 900°C for a few milliseconds or seconds during ethane/propane steam-cracking for instance. The pressure (and consequently the concentration of hydrocarbons) can also vary in a very large domain, from some millibars to 1000 bar. This diversity of pyrolysis conditions is illustrated in different reviews (e.g. [21, 22]). Free-radical reaction pathways are considered as the dominant mechanisms for pyrolysis reactions of organic materials (e.g. [22-24]). The pyrolysis chemistry of the same reactant (and the main products formed) can largely be modified according to the conditions of the reaction (temperature, pressure and time). The knowledge of the thermal reaction mechanism and the rate

of the different pathways provide means to better understand hydrocarbon pyrolysis as well as valuable information for kinetic modelling.

The study of the pyrolysis of *n*-alkanes is simpler than that of other hydrocarbons or organic components. It is rather well known because it has been widely studied for a long time (e.g. [24-34]). Except for methane, the pyrolysis of alkanes consists of free-radical chain reactions. The chemistry is similar whatever the size of the alkane, yet the number of products formed (and the size of the reaction mechanism) increases with the number of carbon atoms of the molecule. At low and usual pressure (0.1-10 bar), the pyrolysis of an alkane produces 1-alkenes and smaller alkanes or hydrogen by cracking reaction. For example, the pyrolysis of propane leads to two main stoichiometric equations:

$$C_3H_8 = C_2H_4 + CH_4$$

$$C_3H_8 = C_3H_6 + H_2$$

This reaction is used for olefin production by steam-cracking for instance.

In petroleum geochemistry, at high pressure (P>100bar) and low temperature (200<T<500°C), several alkanes were chosen as model molecules of the alkane family in oils. For instance, *n*-hexane was chosen [28-29], as well as *n*-pentacosane [35], *n*-hexadecane [36-38] and *n*-octane [39]. In HP-LT (High Pressure-Low Temperature) conditions, the pyrolysis of alkanes is a long chain radical-reaction with two major types of propagation chains: a cracking chain and an alkylation one.

In HP-LT conditions, the detailed kinetic model of alkane pyrolysis was already investigated by several authors (e.g. [24, 29, 40-42]). Therefore, only the major aspects will be recalled here. The pyrolysis of an alkane (here called « μH » [40]) can be schematized by the following free-radical cracking mechanism where μ· and β· are free radicals.

Each cracking propagation chain includes two steps: a decomposition reaction by β-scission and an H-transfer reaction:

Cracking chain:

$$\begin{cases} \mu\cdot \rightarrow \textbf{alkene} + \beta\cdot \\ \beta\cdot + \textbf{μH} \rightarrow \textbf{alkane-minus} + \mu\cdot \end{cases}$$

The corresponding cracking stoichiometric equation (I) is:

$$\textbf{μH = alkane-minus + alkene}$$

where $\beta\cdot$ is a radical lighter than $\mu\cdot$, and « alkane-minus » is an alkane lighter than the reactant μH.

The alkylation propagation chains include two types of free radical reactions: additions of $\mu\cdot$ radicals to alkenes and H-transfers:

Alkylation chain:

$$\begin{cases} \mu\cdot + \textbf{alkene} \rightarrow \mu\text{-alk-plus}\cdot \\ \mu\text{-alk-plus}\cdot + \textbf{μH} \rightarrow \textbf{alkane-plus} + \mu\cdot \end{cases}$$

It leads to the alkylation stoichiometric equation (II):

$$\textbf{alkene + μH = alkane-plus}$$

where μ-alk-plus· is a radical heavier than $\mu\cdot$, and « alkane-plus » is the corresponding alkane which is heavier than the reactant μH.

At low temperature, the addition reactions are fast and the alkylation chains become important, because the activation energy of the additions is particularly low (about 25-34 kJ/mol). So the alkenes become minor products and the global (I + II) stoichiometric equation is:

$$\textbf{μH + μH = alkane-minus + alkane-plus}$$

Isomerization reactions also play an important role in product distribution. They can be unimolecular (1,4 and 1,5 H shift isomerization) and bimolecular by H-transfers between the reactant μH and one of its associated radicals $\mu_i\cdot$ leading to another isomer radical $\mu_j\cdot$:

$$\mu_i\cdot \rightleftharpoons \mu_j\cdot$$

$$\mu_i\cdot + \mu H \rightleftharpoons \mu_j\cdot + \mu H$$

We already studied and modelled the pyrolysis at high pressure (700 bar) and low temperature (300-400°C) of *n*-octane [39] and hexadecane [36-38]. The mechanisms described above lead to modelling results consistent with the experimental ones and they are therefore considered as sufficiently complete (meaning that no major reaction was missing).

For *n*-octane pyrolysis, there are 4 radicals μ_i· (i = 1 to 4, Figure 1) and 6 stoichiometric equations. The major products are:

- 6 "alkane-minus": CH_4 to C_6H_{14}
- 6 "alkane-plus": $C_{10}H_{22}$ to $C_{15}H_{32}$

and the alkenes are minor products : C_2H_4 to C_7H_{14}

The objective of this work is to provide background information on the radical reactions occurring during the pyrolysis of *n*-octane at very low reactant concentration (1 mbar diluted in inert gas - total pressure 1500 mbar - molar fraction 0.07%). It is to be noted that the pressure dependence of rate constant ("fall-off") [e.g. 23] is not studied here, because the total pressure is always above 1 bar. These results are used for constructing a kinetic model. Conditions of low reactant concentration (≤ 10 mbar of partial pressure) can be found in various processes or natural conditions: unburned gas and pollutants in fumes [43, 44], low pressure plasmas, chemical vapor deposition (CVD) [45-48], very low pressure pyrolysis (VLPP) studies [25-28], atmospheric chemistry (earth or other planets) [49, 50], etc.

2. Experimental technique

The experimental pyrolysis study of *n*-octane has been performed in gas phase at very low reactant pressure (1 mbar) in a closed reactor (1 L) made of Pyrex. The *n*-octane is diluted in argon and the total pressure is close to 1500 mbar. Special care was taken to avoid oxygen traces. The temperatures range between 350°C and 450°C and the reaction time from 1 h to 70 h. The analysis was performed by two on-line gas chromatographs. Figure 2 shows the flow sheet of the experimental apparatus.

The experimental setup is connected to a vacuum pump (< 10^{-3} mbar). The gases are introduced in the reactor via a round-bottomed flask (2 L) which allows the mixing of the reactant and the inert gas (argon). The liquid reactant (*n*-octane) is introduced by a syringe through a double septum, protected from the air by a flow of argon. The amount of reactant is very small (10-50 µL), as to ensure that it is totally vaporized in the mixer which is under vacuum (<10^{-3} mbar). Inert gas is introduced by a central injector equipped with 4 nozzles in order to homogenize the mixture. The total pressure in the mixer reaches 2-3 bar, which allows the expansion of the gas toward the reactor in a second step.

The main three steps of an experiment are:

- pumping of all experimental setup and heating of the empty reactor,
- mixing of the reactant-argon mixture in the mixer and waiting for the homogenization during 10 min,
- expansion of the gases toward the reactor and beginning of the thermal reaction.

During the same experiment, an aliquot fraction is removed at different reaction times from the reactor by expansion toward the heated analysis line. The amount of the aliquot fraction is very small and controlled by the pressure in the reactor (maximum drop of pressure = 20 mbar). The pressure drops are small in regards to the total pressure in the reactor (1500 mbar). Therefore, several aliquot fractions can be removed from the reactor without disturbing the reaction.

The analysis of the reactant and the products is performed by two online Gas Chromatographs. The chromatograph HEWLETT-PACKARD HP 6850 is equipped with a FID and a semi-capillary column (GS-Alumina, length 30 m, diameter 0.53 mm). The temperature program of the oven is as follows: the initial temperature is set at 40°C during 10 min, then a heating rate of 10 °C/min is applied up to 190°C, and the final temperature is kept at 190°C during 20 min. This allows the analysis of the light alkanes and alkenes (from C_1 to C_8). In this setup, hydrogen cannot be measured.

The chromatograph SHIMADZU GC 17 is equipped with a FID and a packed column (Alltech,

158 length 3.6 m, stationary phase: 35% BCEF – 10% OV 101), which works isothermally at 50°C.
159 It is particularly well adapted to the analysis of the heavy alkanes from C_9 to C_{15}, but none of
160 them was detected in the entire study. The GC calibrations were performed by using several
161 standard mixtures.
162 All data presented in this paper were generally verified by three or four sets of GC data. The
163 repeatability for the molar fractions is usually less than 5% for the major products. The carbon
164 balance is typically 1±0.05 and the C/H ratio remains quite constant (between 0.40 and 0.44 at
165 400°C and between 0.44 and 0.47 at 450°C).

166 **3. Experimental results**

167 The major products obtained are methane, ethane and 1-alkenes (C_2H_4 to C_7H_{14}). Figures 3 show
168 the evolution of conversion versus reaction time at different temperatures.
169 At 450°C and 4 h, the *n*-octane conversion is greater than 8% and the three main reaction
170 products are ethylene, propene and methane, with molar fractions ranging in the following order:

171 $$C_2H_4 > C_3H_6 \cong CH_4$$

172 followed by higher alkenes and ethane:

173 $$C_4H_8 > C_5H_{10} > C_6H_{12} \cong C_2H_6 > C_7H_{14}$$

174 The minor products observed are alkanes from C_3H_8 to C_7H_{16}.
175 The evolution of products versus reaction time will be detailed beneath in section 5 dedicated to
176 the modeling. Figure 4 represents the global evolution of alkanes-minus and alkenes that are the
177 two families of products.
178 It should be noted that these experimental results are very different from the thermal
179 decomposition of *n*-alkanes at the same low temperature but at high pressure [39]. In particular,
180 the cracking stoichiometric equations (for example: $C_8H_{18} = C_2H_4 + C_6H_{14}$) are not observed
181 since C_3^+ alkanes are in very low quantities and the alkylation stoichiometric equation (for
182 example: $C_8H_{18} + C_2H_4 = C_{10}H_{22}$) are negligible: alkenes are important and alkanes-plus (C_8^+) are

not detected. The experimental results at 450°C are given in Table 1 and the details as Supplementary Materials.

4. Discussion: kinetic mechanism of *n*-octane pyrolysis at very low concentration

In comparison with the study of the pyrolysis of *n*-octane at 700 bar [39], the range of temperature is the same (350-450°C), but the reactant partial pressure (1 mbar) is very different, the initial concentration of reactant being lower by more than a factor of 10^5. The very low concentration of reactant (called μH) minimizes the importance of the bimolecular reactions in the mechanism, in particular the H-transfer in the cracking propagation chain:

$$\begin{cases} \mu\cdot \rightarrow \text{alkene} + \beta\cdot & \text{(decomposition by β-scission)} \\ \beta\cdot + \mu H \rightarrow \beta H + \mu\cdot & \text{(H-transfer)} \end{cases}$$

In our low concentration conditions, the radicals are decomposed by β-scission of C-C bonds as much as possible (unimolecular reaction), rather than reacting by H-transfer with the reactant (bimolecular reaction, which produces an alkane). The methyl and ethyl radicals cannot be decomposed by β-scission of C-C bonds, so they react by H-transfer with the reactant and produce methane or ethane and μ· which is the chain carrier radical. At low temperature and low pressure, the cracking propagation chain becomes:

$$\begin{cases} \mu\cdot \rightarrow \text{alkene-1} + \beta\cdot \\ \beta\cdot \rightarrow \text{alkene-2} + \beta_i\cdot \\ \beta_i\cdot \rightarrow \text{alkene-3} + \beta_j\cdot \quad \text{and when } \beta_j\cdot = CH_3\cdot \text{ or } C_2H_5\cdot, \\ CH_3\cdot \text{ or } C_2H_5\cdot + \mu H \rightarrow CH_4 \text{ or } C_2H_6 + \mu\cdot \end{cases}$$

For the *n*-octane pyrolysis, there are 4 $\mu_i\cdot$ radicals (Figure 1), which lead to 4 cracking

propagation chains and 4 stoichiometric equations.

From $\mu_1^{\cdot}$ radical, the low pressure propagation chain is:

$$\mu_1^{\cdot} \rightarrow C_2H_4 + C_6H_{13}^{\cdot}$$

$$C_6H_{13}^{\cdot} \rightarrow C_2H_4 + C_4H_9^{\cdot}$$

$$C_4H_9^{\cdot} \rightarrow C_2H_4 + C_2H_5^{\cdot}$$

$$C_2H_5^{\cdot} + C_8H_{18} \rightarrow C_2H_6 + \mu^{\cdot} \text{ (all } \mu_i^{\cdot} \text{ radicals, including } \mu_1^{\cdot})$$

The corresponding cracking stoichiometric equation is:

$$\mathbf{C_8H_{18} = 3\ C_2H_4 + C_2H_6} \qquad \text{(I')}$$

From $\mu_2^{\cdot}$ radical, an equivalent propagation chain leads to the stoichiometric equation:

$$\mathbf{C_8H_{18} = C_3H_6 + 2\ C_2H_4 + CH_4} \qquad \text{(II')}$$

In the case of $\mu_3^{\cdot}$, there are two possibilities of C-C bond scission:

$$\mu_3^{\cdot} \rightarrow C_7H_{14} + CH_3^{\cdot}$$

and $$\mu_3^{\cdot} \rightarrow C_4H_8 + C_4H_9^{\cdot}$$

These chain reactions lead to the following stoichiometric equations:

$$\mathbf{C_8H_{18} = CH_4 + C_7H_{14}} \qquad \text{(III'a)}$$

$$\mathbf{C_8H_{18} = C_4H_8 + C_2H_4 + C_2H_6} \qquad \text{(III'b)}$$

In the $\mu_4^{\cdot}$ radical, there are also two possibilities of C-C bond scission and the stoichiometric equations are:

$$\mathbf{C_8H_{18} = C_6H_{12} + C_2H_6} \qquad \text{(IV'a)}$$

$$\mathbf{C_8H_{18} = C_5H_{10} + C_2H_4 + CH_4} \qquad \text{(IV'b)}$$

So, the stoichiometric equations lead to the formation of two alkanes, CH_4 and C_2H_6, and all alkenes from C_2 to C_7. This well agrees with the main products observed when the pyrolysis of *n*-octane is performed at very low reactant concentration.

If we suppose, in a first approximation, that all the cracking stoichiometric equations have the same rate, the global stoichiometric equation is:

$$\mathbf{6\ C_8H_{18} = 7\ C_2H_4 + 3\ CH_4 + 3\ C_2H_6 + C_3H_6 + C_4H_8 + C_5H_{10} + C_6H_{12} + C_7H_{14}}$$

That leads to the following classification:

$C_2H_4 > CH_4 = C_2H_6 > C_3H_6 = C_4H_8 = C_5H_{10} = C_6H_{12} = C_7H_{14}$ (without alkanes in C_{3+})

The classification has to be compared with our experimental results at 450°C and 4 h (Figures 5 and 6):

$C_2H_4 > CH_4 \approx C_3H_6 > C_4H_8 > C_5H_{10} \approx C_6H_{12} > C_2H_6 > C_7H_{14} >> C_3H_8$, C_4H_{10}, C_5H_{12}, C_6H_{14} and C_7H_{16}

The little quantitative differences between the experimental classification and the classification obtained by the stoichiometric equations could be explained by three approximations. First, the concentrations of the $\mu_i^{\cdot}$ are not equal, because $\mu_1^{\cdot}$ is a primary radical which is less stable than a secondary one:

$[\mu_1^{\cdot}] < [\mu_2^{\cdot}] \sim [\mu_3^{\cdot}] \sim [\mu_4^{\cdot}]$

Consequently, the stoichiometric equation I' (leading to C_2H_6) is overestimated in the argument which only considers the stoichiometric equations.

Another correction is that the decompositions by β-scission of C-H bonds are not completely negligible at 450°C. They lead to the conversion of ethane into ethylene, which is the major product:

$C_2H_5^{\cdot} \rightarrow C_2H_4 + H^{\cdot}$

$H^{\cdot} + C_8H_{18} \rightarrow H_2 + \mu^{\cdot}$

Finally, the formation of C_3^+ alkanes in very low quantities indicates that the H transfer reactions of $\beta^{\cdot}$ radicals (C_3-C_6 radicals) are not totally negligible and produce C_3^+ alkanes:

$\beta^{\cdot} + \mu H \rightarrow C_{3+}$ alkanes $+ \mu^{\cdot}$

This brief kinetic interpretation well explains the chemistry observed for the *n*-octane pyrolysis at low reactant concentration and low temperature, and the differences in the product distribution obtained at high concentration and pressure (competition: unimolecular versus bimolecular reactions).

5. Modeling of *n*-octane thermal decomposition at very low reactant concentration.

On the basis of these free-radical reactions, a systematic approach is used to build a detailed mechanism of *n*-octane pyrolysis at low reactant concentration and low temperature. Using EXGAS software [40, 51], the mechanism (primary and partial secondary) is made of 184 reactions involving 34 species (16 molecules and 18 radicals). The kinetic data originate from NIST Database [52] or literature and are summarized in [40]. The simulations are performed using Chemkin II software [53], in a closed isochoric and isothermal reactor (Senkin).

The comparison between the experimental results and simulation ones led to the adjustment of some rate constants by a minor factor (less or equal to 10) in order to better account for main pyrolysis products. Figures 5, 6 and 7 present the comparison between the experimental data and the simulation results of the molar fractions (*n*-octane and reaction products) versus time (1 to 240 minutes) at 450°C and 1 mbar of *n*-octane partial pressure (total pressure 1500 mbar - molar fraction 0.07%).

The detailed kinetic model accounts for the nature of the products observed as well as for their amounts, at least semi-quantitatively. The evolution of alkenes, *n*-octane and propane is well simulated by the kinetic model, although ethene is very slightly over-estimated, and pentene and hexene are under-estimated, but they are minor products. The overestimation of ethene can be due to additions of some radicals to alkenes, which are secondary reactions not taken into account by the model. Methane and ethane are also very slightly overestimated by the model, probably for the same reason, because methyl and ethyl radicals are the predominant radicals. In the case of ethane, this may also be due to the decomposition of C-H bonds, which is not completely negligible at 450°C and leads to the conversion of ethane into ethylene. Nevertheless we can therefore conclude that the kinetic model is globally validated as well as the kinetic scheme proposed to explain the chemistry observed at very low concentration.

By simulation of the kinetic model, the chain length can be estimated by the ratio of the global propagation rate to the initiation rate. The main H-transfers with *n*-octane are those implying the

methyl and ethyl radicals. The chain length is equal to 120 at 450°C and low *n*-octane concentration (molar fraction 0.07%). The chain length increases when the temperature decreases and in our conditions, the chain length is always very high.

When a reaction follows a first order kinetic law, the plot of log (1-conversion) versus time must give a linear relationship and the slope corresponds to the rate constant. Assuming a first order kinetics, we can estimate the apparent activation energy of *n*-octane pyrolysis: it is close to 218 kJ/mol and the frequency factor is about 3.63×10^{10} (s^{-1}), in the range 350°C – 450°C and 1 mbar of *n*-octane partial pressure. This apparent activation energy is lower than that of alkane pyrolysis at the same temperatures but at high pressure (100-700 bar), which is close to 284-289 kJ/mol [35, 39, 42, 54].

This difference can be explained by the concentration of reactant that is totally different in our case in comparison to those applied in [35, 39, 42]. The elementary reactions that are important, are also different, depending on the reaction conditions. Indeed, in the chain propagation, the H-transfers of radicals with reactant, which produce smaller alkanes than the reactant, are in competition with the decomposition of this radical by β-scission which produce smaller alkenes:

$$\beta\cdot \rightarrow \textbf{alkene} + \beta'\cdot$$

$$\beta\cdot + \mu H \rightarrow \textbf{alkane } \boldsymbol{\beta H} + \mu\cdot$$

At very low reactant concentration, unimolecular decomposition reactions are greatly favored over bimolecular reactions, and that leads to very different apparent activation energies.

6. Conclusion

An experimental study of the pyrolysis of *n*-octane has been performed at very low reactant concentration (1 mbar diluted in inert gas - total pressure 1500 mbar - molar fraction 0.07%) in a closed reactor, at temperatures between 350°C and 450°C and reaction time from 1 h to 70 h. The major products of the reaction are 1-alkenes (C_2H_4 to C_7H_{14}), methane and ethane. These experimental results are different from the thermal decomposition of *n*-octane at the same low

313 temperature but at high pressure (the major products are only alkanes at 700 bar).

314 Indeed, at very low reactant concentration, unimolecular decomposition reactions are greatly
315 favored over bimolecular reactions. In our low concentration conditions, radicals decompose
316 several times by β-scission of C-C bonds as much as possible (unimolecular reaction), rather
317 than react by H-transfer with the reactant (bimolecular reaction) which produces an alkane. The
318 methyl and ethyl radicals cannot decompose by C-C β-scission, and so they react by H-transfer
319 with the reactant and produce methane or ethane and μ·, which is the chain carrier radical.

320

321 On the basis of these free-radical reactions, a detailed kinetic model (184 reactions, 16 molecules
322 and 18 radicals) is proposed, which allows a satisfying description of the experimental results:

323 - the nature of the principal reaction products is correct,

324 - C_2H_4 is the most important product,

325 - CH_4 and C_2H_6 are the only two important alkanes,

326 - the alkenes from C_3 to C_7 are formed in rather close quantities,

327 - the C_3^+ alkanes are very minor products.

328 These results of *n*-octane pyrolysis obtained at very low reactant concentration underline the
329 crucial role of concentration and partial pressure in the reaction pathways and products of the
330 alkane pyrolysis. They clearly demonstrate that results obtained at low partial pressure cannot be
331 extrapolated at high pressure and vice versa.

332

333

334 REFERENCES

335

336 [1] M. Vandenbroucke, F.Behar, J.L. Rudkiewicz, Kinetic modelling of petroleum formation and
337 cracking: implications from the high pressure/high temperature Elgin Field (UK, North Sea),
338 Org. Geochem. 30 (9) (1999) 1105–1125.

339 [2] K.E. Peters, M.G. Fowler, Applications of petroleum geochemistry to exploration and
340 reservoir management, Org. Geochem. 33 (1) (2002) 5–36.

341 [3] R.J. Hill, Y. Tang, I.R. Kaplan, Insights into oil cracking based on laboratory experiments,
342 Org. Geochem. 34 (12) (2003) 1651-1672.

343 [4] M. Bajus, V.C. Vesela, P.A. Leclercq, J.A. Rijks, Steam Cracking of Hydrocarbons. 2.
344 Pyrolysis of Methylcyclohexane, Ind. Eng. Chem. Prod. Res. Dev 18 (1) (1979) 135-142.

345 [5] G.F. Froment, Kinetics and reactor design in the thermal cracking for olefins production,
346 Chem. Eng. Sci. 47 (9-11) (1992) 2163–2177.

347 [6] S.M. Sadrameli, A.E.S. Green, Systematics and modeling representations of naphtha thermal
348 cracking for olefin production, J. Anal. Appl. Pyrolysis, 73 (2) (2005) 305–313.

349 [7] K. M. Van Geem, D. Hudebine, M.F. Reyniers, F.Wahl, J. Verstraete, G. B. Marin,
350 Molecular reconstruction of naphtha steam cracking feedstocks based on commercial indices,
351 Comput. Chem. Eng., 31 (9) (2007) 1020–1034.

352 [8] T. Edwards, Cracking and deposition behavior of supercritical hydrocarbon aviation fuels,
353 Combust. Sci. Tech., 178 (1-3) (2006) 307–334.

354 [9] O. Herbinet, B. Sirjean, R. Bounaceur, R. Fournet, F. Battin-Leclerc, G. Scacchi, P.M.
355 Marquaire, Primary reactions of the thermal decomposition of tricyclodecane, J. Phys. Chem. A,
356 110 (39) (2006) 11298-11314.

357 [10] N. Vandewiele, G. Magoon, K. Van Geem, M.F. Reyniers, W. Green, G. Marin, Kinetic
358 Modeling of Jet Propellant-10 Pyrolysis, Energy Fuels, 29 (1) (2015) 413–427.

359 [11] P.R. Solomon, M.A. Serio, G.V., Despande, E. Kroo, Cross-linking reactions during coal

conversion, Energy Fuels 4 (1) (1990) 42–54.

[12] S. Wang, H. Huang, K. Wang, M.T. Klein, W.H. Calkins, Kinetics of Coal Liquefaction Distillation Resid Conversion, Energy Fuels, 12 (6) (1998) 1335–1341.

[13] N. Howaniec, A. Smoliński, Effect of fuel blend composition on the efficiency of hydrogen-rich gas production in co-gasification of coal and biomass, Fuel 128 (2014) 442-450.

[14] J.G. Speight, Coal gasification processes for synthetic liquid fuel production, in: R. Luque, J. Speight (Eds.), Gasification for Synthetic Fuel Production - Fundamentals, Processes and Applications, Woodhead Publishing Series in Energy, Elsevier Ltd, 2015.

[15] W. Kaminsky, B. Schlesselmann, C. Simon, Olefins from polyolefins and mixed plastics by pyrolysis, J. Anal. Appl. Pyrol. 32 (1995) 19–27.

[16] A. Uddin, K. Koizumi, K. Murata, Y. Sakata, Thermal and catalytic degradation of structurally different types of polyethylene into fuel oil, Polym. Degrad. Stab. 56 (1) (1997) 37–44.

[17] E. Hajekova, M. Bajus, Recycling of low-density polyethylene and polypropylene via copyrolysis of polyalkene oil/waxes with naphtha: product distribution and coke formation, J. Anal. Appl. Pyrolysis 74 (1-2) (2005) 270–281.

[18] I. Ziegler, R. Fournet, P.M.Marquaire, Pyrolysis of propane for CVI of pyrocarbon - part I: Experimental and modeling study of the formation of toluene and aliphatic species, J. Anal. Appl. Pyrol. 73(2) (2005) 212-230.

[19] I. Ziegler, R. Fournet, P.M. Marquaire, Pyrolysis of propane for CVI of pyrocarbon - part II: Experimental and modeling study of polyaromatic species, J. Anal. Appl. Pyrol. 73(2) (2005) 231-247.

[20] R. Lacroix, R. Fournet, I. Ziegler-Devin, P.M. Marquaire, Kinetic Modeling of Surface Reactions Involved in CVI of Pyrocarbon obtained by propane pyrolysis, Carbon 48 (1) (2010)132-144.

[21] S. Moldoveanu, Pyrolysis of organic molecules-Applications to Health and Environmental

386 Issues, first ed., Elsevier, 2009.
387 [22] P.E. Savage, Mechanisms and kinetics models for hydrocarbon pyrolysis, J. Anal. Appl.
388 Pyrolysis 54 (1-2) (2000) 109–126.
389 [23] K.J. Laidler, L.F Louks, Comprehensive Chemical Kinetics, vol 5, Elsevier, 1972.
390 [24] M.L. Poutsma, Fundamental reactions of free radicals relevant to pyrolysis reactions, J.
391 Anal. Appl. Pyrolysis 54 (1-2) (2000) 5–35.
392 [25] F. O. Rice, K. F. Herzfeld, The Thermal Decomposition of Organic Compounds from the
393 Standpoint of Free Radicals. VI. The Mechanism of Some Chain Reactions, J. Am. Chem. Soc.,
394 56 (1934) 284-289.
395 [26] D.L.Allara, R. Shaw, A compilation ok kinetic-parameters for the thermal degradation of
396 normal-alkane molecules, J. Phys. Chem. Ref. Data, 9 (3) (1980) 523-559.
397 [27] T. J. Ford, Liquid-Phase Thermal Decomposition of Hexadecane: Reaction Mechanisms,
398 Ind. Eng. Chem. Fundam., 25 (2) (1986) 240-243.
399 [28] F. Dominé, Kinetics of hexane pyrolysis at very high pressures. 1. Experimental study,
400 Energy Fuels 3 (1) (1989) 89–96.
401 [29] F. Dominé, P.M. Marquaire, C. Muller, G.-M. Côme, Kinetics of hexane pyrolysis at very
402 high pressures. 2. Computer modeling, Energy Fuels 4(1) (1990) 2–10.
403 [30] F. Khorasheh, M. R. Gray, High-Pressure Thermal Cracking of *n*-Hexadecane, Ind. Eng.
404 Chem. Res., 32 (9) (1993) 1853-1863.
405 [31] K.J. Jackson, A.K. Burnham, R.L. Braun, K.G. Knauss, Temperature and pressure
406 dependence of n-hexadecane cracking, Org. Geochem. 23 (10) (1995) 941–953.
407 [32] O. Herbinet, PM. Marquaire, F. Battin-Leclerc, R. Fournet, Thermal stability of *n*-dodecane:
408 experiments and kinetic modeling, J. Anal. Appl. Pyrol., 78(2) (2007) 419-429.
409 [33] M. J. De Witt, D. J. Dooling, L J. Broadbelt, Computer Generation of Reaction Mechanisms
410 Using Quantitative Rate Information: Application to Long-Chain Hydrocarbon Pyrolysis, Ind.
411 Eng. Chem. Res. 39 (2000) 2228-2237.

412 [34] J. Yu, S. Eser, Kinetics of Supercritical-Phase Thermal Decomposition of C10−C14 Normal
413 Alkanes and Their Mixtures Ind. Eng. Chem. Res. 36 (3) (1997) 585–591.
414 [35] F. Behar, M. Vandenbroucke, Experimental Determination of the Rate Constants of the *n*-
415 C25 Thermal Cracking at 120, 400, and 800 bar: Implications for High-Pressure/High-
416 Temperature Prospects, Energy Fuels 10 (4) (1996) 932-940.
417 [36] R. Bounaceur, G. Scacchi, P.M. Marquaire, F. Dominé, D. Dessort, B. Pradier, Inhibiting
418 effect of tetralin on the pyrolytic decomposition of hexadecane. Comparison with toluene, Ind.
419 Eng. Chem. Res. 41 (19) (2002) 4689–4701.
420 [37] V. Burklé-Vitzthum, R. Michels, G. Scacchi, P.M. Marquaire, D. Dessort, B. Pradier, O.
421 Brevart, Kinetic effect of alkylaromatics on the thermal stability of hydrocarbons under
422 geological conditions, Org. Geochem. 35 (1) (2004) 3-31.
423 [38] V. Burklé-Vitzthum, R. Michels, R. Bounaceur, P.M. Marquaire, G. Scacchi, Experimental
424 study and modeling of the role of hydronaphthalenics on the thermal stability of hydrocarbons at
425 laboratory and geological conditions, Ind. Eng. Chem. Res. 44 (24) (2005) 8972-8987.
426 [39] F. Lannuzel, R. Bounaceur, R. Michels, G. Scacchi, P.M. Marquaire, Reassessment of the
427 kinetic influence of toluene on *n*-alkanes pyrolysis, Energy Fuels 24 (7) (2010) 3817-3830.
428 [40] R. Bounaceur, V. Warth, P. M. Marquaire, G. Scacchi, F. Dominé, D. Dessort, B. Pradier,
429 O. Brevart, Modeling of hydrocarbons pyrolysis at low temperature. Automatic generation of
430 free radicals mechanisms, J. Anal. Appl. Pyrolysis 64 (2002) 103-122.
431 [41] F. Dominé, R. Bounaceur, G. Scacchi, P.M. Marquaire, D. Dessort, B. Pradier, O. Brévart,
432 Up to what temperature is petroleum stable ? New insights from a 5200 free radical reactions
433 model, Org. Geochem. 33 (12) (2002) 1487-1499.
434 [42] V. Burklé-Vitzthum, R. Bounaceur, P-M. Marquaire, F. Montel, L. Fusetti, Thermal
435 evolution of *n*- and iso-alkanes in oils - Part 1: Pyrolysis model for a mixture of 78 alkanes (C1-
436 C32) including 13,206 free radical reactions, Org. Geochem. 42 (5) (2011) 439-450.
437 [43] I. Ziegler-Devin, R. Bounaceur, C. Perrin, R. Wörner, F. Patisson, P. M. Marquaire, Kinetic

438 study of abatement of low concentration of dibenzofuran by oxidation – Effects of co-reactants,
439 Chem. Eng. J. 218 (2013) 154-163.
440 [44] A. Tritz, I. Ziegler-Devin, C. Perrin, P.M. Marquaire, Experimental study of the oxidation
441 and pyrolysis of dibenzofuran at very low concentration, J. Env. Chem. Eng., 2 (2014) 143-153.
442 [45] G. Vignoles, F. Langlais, C. Descamps, A. Mouchon, H. Le Poche H, N. Reuge, CVD and
443 CVI of pyrocarbon from various precursors, Surf. Coat. Technol. 188-189 (2004) 241–249.
444 [46] K. Norinaga, O. Deutschmann, Detailed kinetic modeling of gas-phase reactions in the
445 chemical vapor deposit of carbon from light hydrocarbons, Ind. Eng. Chem. Res. 46 (11) (2007)
446 3547–3557.
447 [47] M. Frenklach, H. Wang, Detailed surface and gas-phase chemical kinetics of diamond
448 deposit, Phys. Rev. B: Condens. Matter, 43 (2) (1991) 1520-1545.
449 [48] S.W. Benson, G. N. Spokes, Very Low Pressure Pyrolysis. III t-butyl hydroperoxide in
450 Fused Silica and Stainless Steel Reactors, J. Phys. Chem. 72 (1968)1182-1186.
451 [49] R. Atkinson, J. Arey, S. M. Aschmann Atmospheric chemistry of alkanes: Review and
452 recent developments Atmospheric Environment, 42 (2008) 5859-5871
453 [50] O. Venot, E. Hébrard, M. Agúndez, L. Decin, R. Bounaceur A new chemical scheme to
454 study carbon-rich exoplanet atmospheres Astronomy & Astrophysics, in press 2015
455 (arXiv:1502.03567)
456 [51] F. Battin-Leclerc, J. Biet, R. Bounaceur, G.M. Côme, R. Fournet, P.-A. Glaude, X.
457 Grandmougin, O. Herbinet, G. Scacchi, V. Warth, EXGAS-ALKANES-ESTERS: A software for
458 the automatic generation of mechanisms for the oxidation of alkanes and esters, (2010) LRGP,
459 UPR CNRS 3349
460 [52] J. A. Manion, R. E. Huie, R. D. Levin, D. R. Burgess Jr., V. L. Orkin, W. Tsang, W. S.
461 McGivern, J. W. Hudgens, V. D. Knyazev, D. B. Atkinson, E. Chai, A. M. Tereza, C.-Y. Lin, T.
462 C. Allison, W. G. Mallard, F. Westley, J. T. Herron, R. F. Hampson, D. H. Frizzell, NIST
463 Chemical Kinetics Database, NIST Standard Reference Database 17, Version 7.0 (Web Version),

Release 1.4.3, Data version 2008.12, National Institute of Standards and Technology, Gaithersburg, Maryland, 20899-8320. http://kinetics.nist.gov

[53] R.J Kee, F.M. Rupley, J.A. Miller, Chemkin-II: A Fortran chemical kinetics package for the analysis of gas-phase chemical kinetics, (1989) Sandia National Laboratories, Livermore, CA.

[54] F. Behar, F. Lorant, L. Mazeas, Elaboration of a new compositional kinetic schema for oil cracking, Org. Geochem. 39 (6) (2008) 764–782.

474 TABLE CAPTION

475

476 **Table 1:** Product distribution in mol. % - Octane pyrolysis at 450°C-initial pressure of octane =

477 1 mbar - total pressure = 1500mbar

478

CH_4	-	9.40×10^{-4}	1.39×10^{-3}	1.87×10^{-3}	2.25×10^{-3}
C_2H_6	-	2.40×10^{-4}	3.21×10^{-4}	4.06×10^{-4}	5.32×10^{-4}
C_3H_8	-	8.07×10^{-6}	1.01×10^{-5}	9.46×10^{-6}	1.31×10^{-5}
C_4H_{10}	-	3.23×10^{-6}	4.90×10^{-6}	4.71×10^{-6}	5.27×10^{-6}
C_2H_4	-	3.28×10^{-3}	4.79×10^{-3}	6.31×10^{-3}	7.56×10^{-3}
C_3H_6	-	1.32×10^{-3}	1.94×10^{-3}	2.65×10^{-3}	3.22×10^{-3}
C_4H_8	-	6.56×10^{-4}	8.85×10^{-4}	1.16×10^{-3}	1.40×10^{-3}
C_5H_{10}	-	5.18×10^{-4}	7.50×10^{-4}	8.74×10^{-4}	9.61×10^{-4}
C_6H_{12}	-	4.94×10^{-4}	6.43×10^{-4}	7.50×10^{-4}	8.60×10^{-4}
C_7H_{14}	-	1.02×10^{-4}	1.43×10^{-4}	2.16×10^{-4}	2.02×10^{-4}
C_8H_{18}	6.65×10^{-2}	6.49×10^{-2}	6.31×10^{-2}	6.21×10^{-2}	6.11×10^{-2}

479

FIGURE CAPTIONS

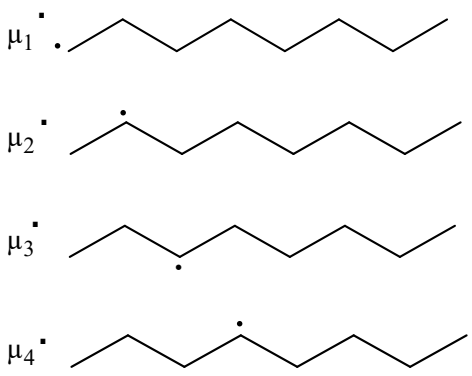

Figure 1. The μ_i· radicals of *n*-octane. Names used in the equations of reactions.

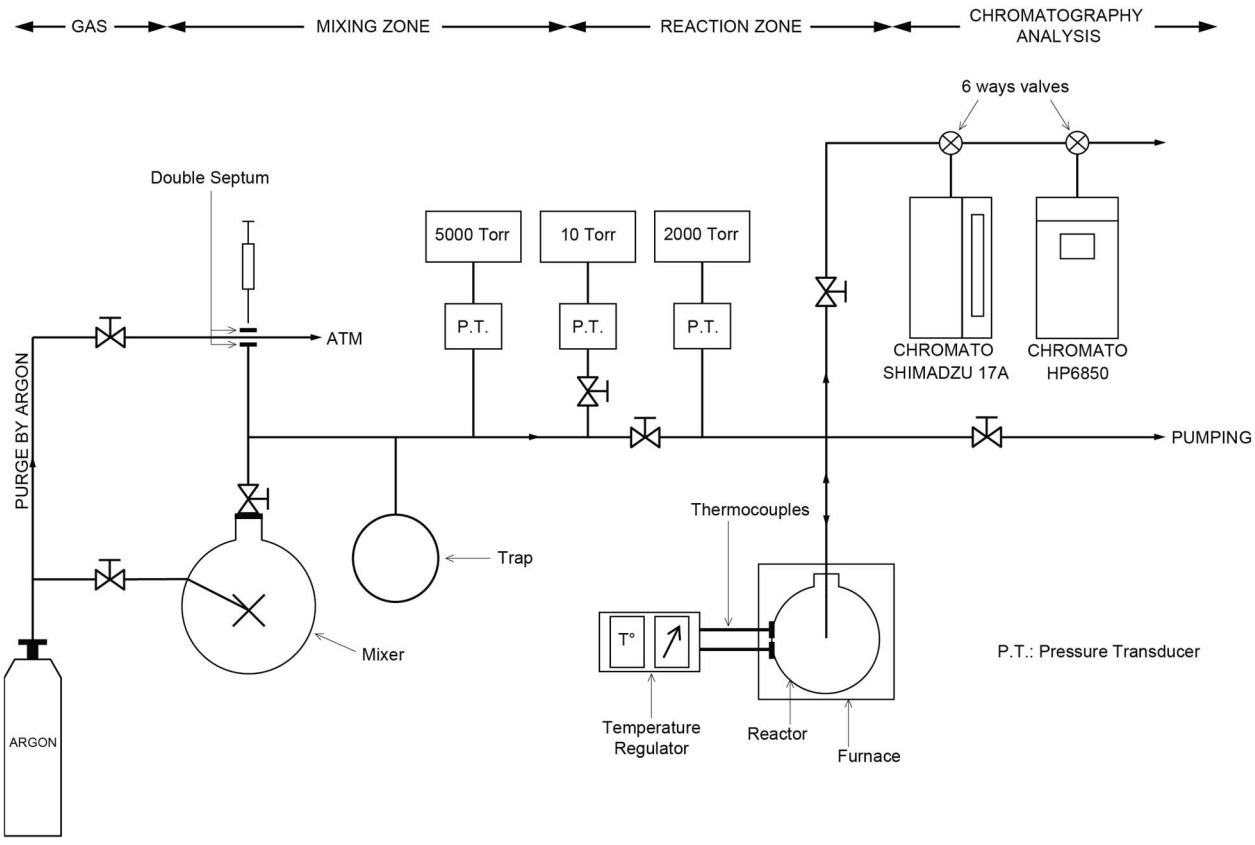

Figure 2. Flow sheet of the experimental setup.

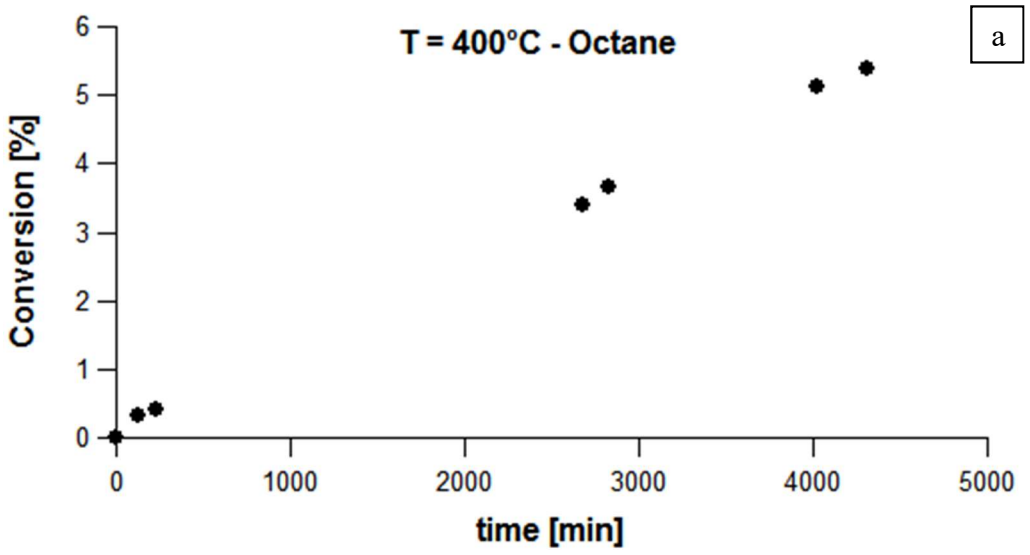

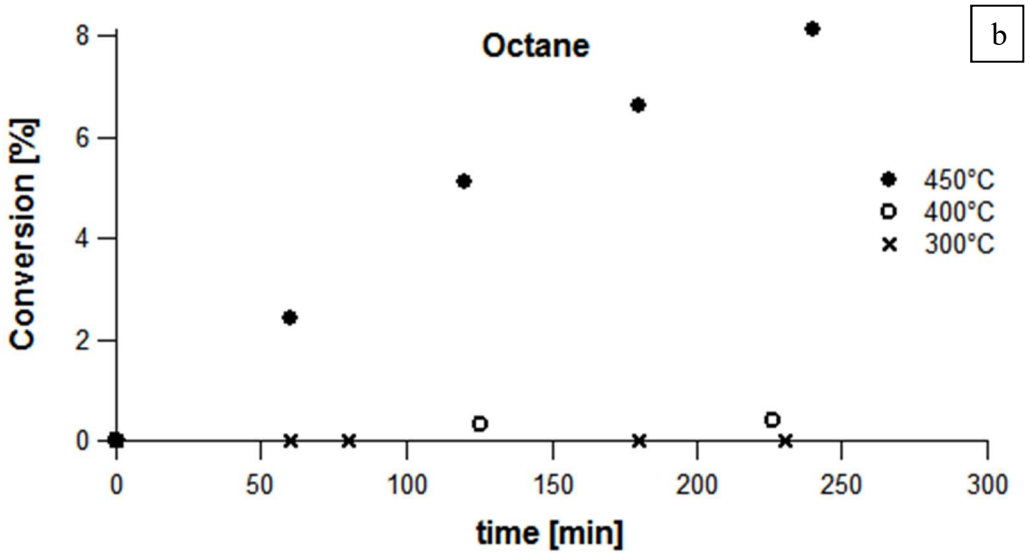

Figures 3. Evolution of *n*-octane conversion as a function of time, a) at 400°C, up to 4300 min, and b) at 350, 400, 450°C, up to 240 min (1mbar initial *n*-octane pressure).

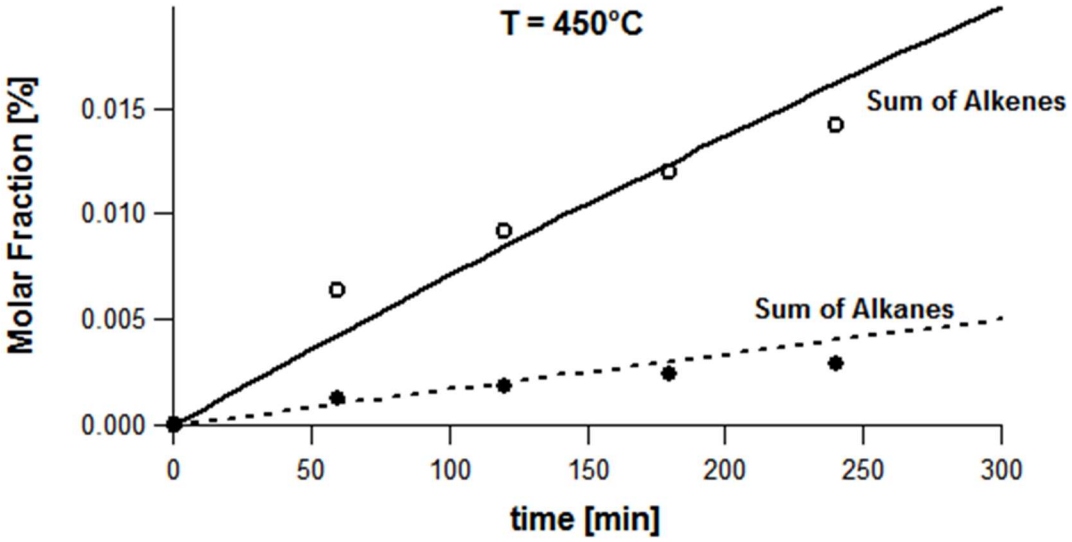

508
509

510 **Figure 4.** Comparison between experimental (dots) and simulation (solid lines) molar fractions
511 of the alkanes-minus and alkenes, as a function of time, at 450°C and 1mbar initial *n*-octane
512 pressure.

513

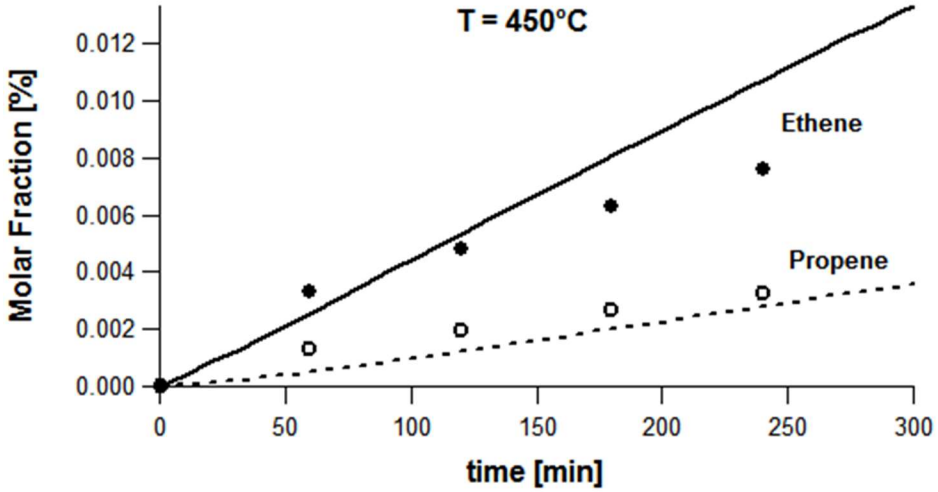

514

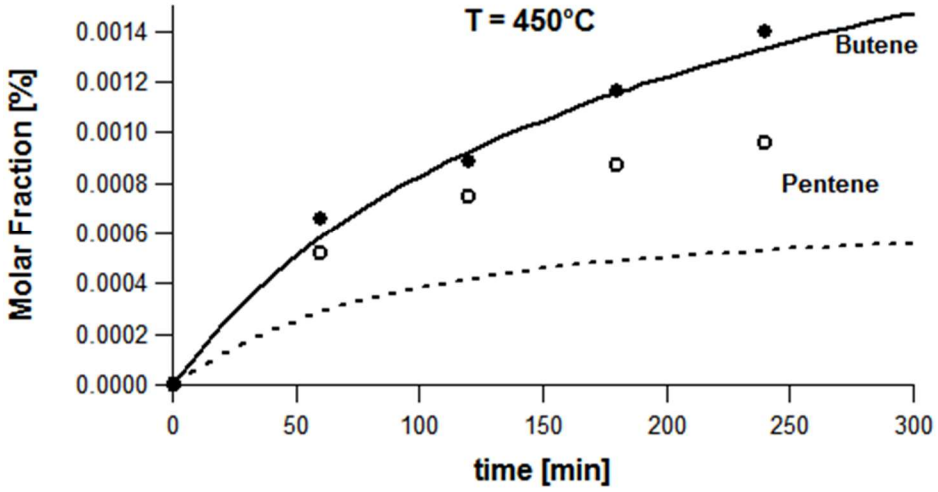

515

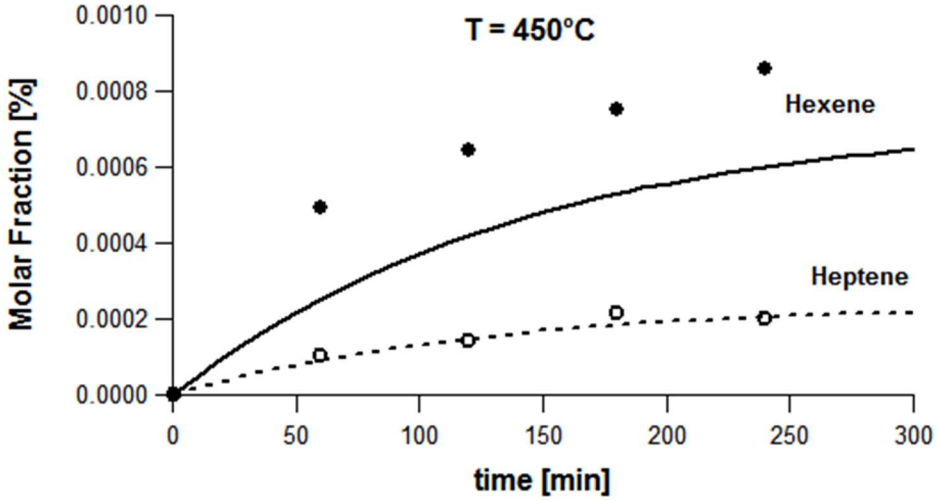

516
517

518

519 **Figures 5.** Comparison between experimental (dots) and simulation (solid lines) molar fractions
520 of the alkenes (from ethylene to heptene), as a function of time, at 450°C and 1mbar initial *n*-
521 octane pressure.

522

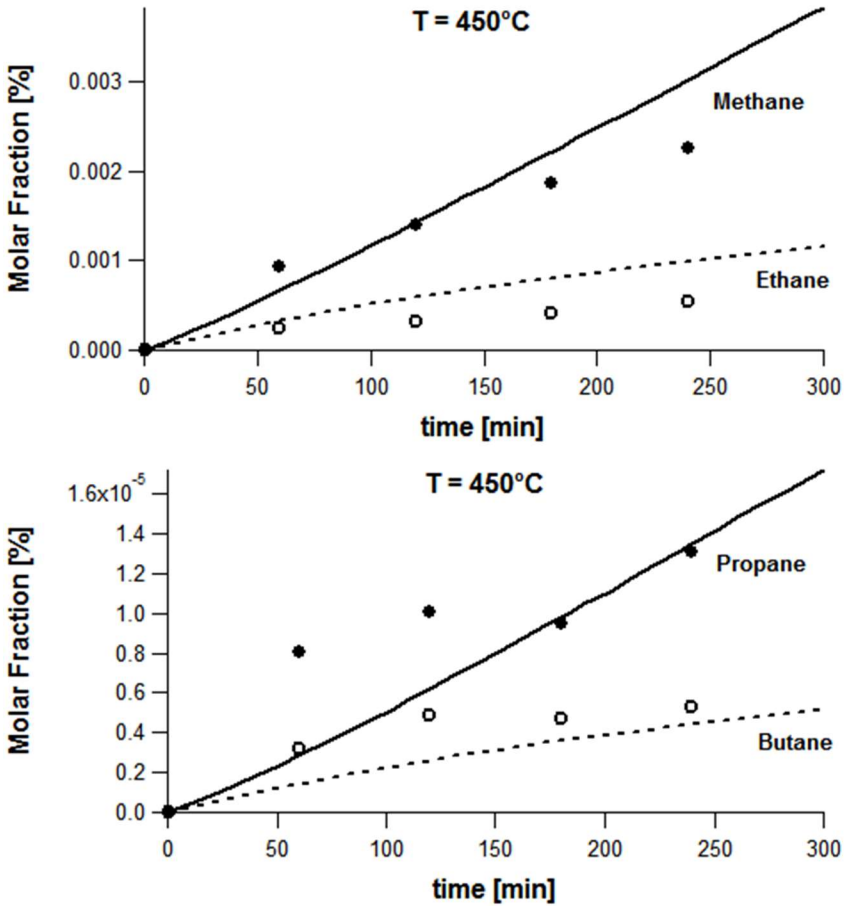

Figures 6. Comparison between experimental (dots) and simulation (solid lines) molar fractions of the alkanes (from methane to butane), as a function of time, at 450°C and 1mbar initial *n*-octane pressure.

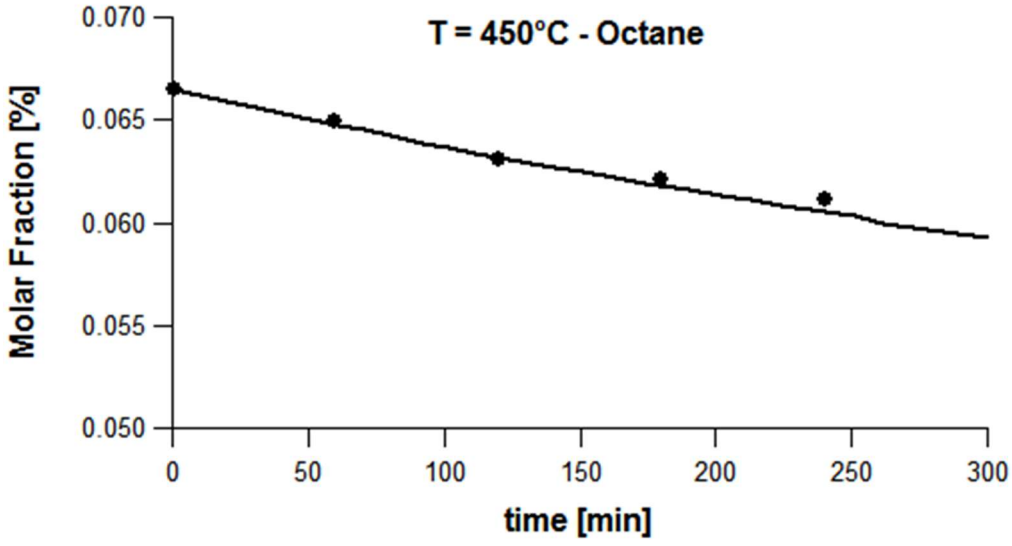

532

533

534 **Figure 7.** Comparison between experimental and simulation molar fraction of *n*-octane, as a
535 function of time, at 450°C and 1mbar initial *n*-octane pressure.

536

537